Removal of *para*-Phenylenediamine (PPD) Dye from Its Aqueous Solution by Adsorption Using the Activated Carbon Nanoparticles

Shahbaa Fayyad Bdewi[1], Hanaa Hassan Hussein[2*], and Shireen Abdulmohsin Azeez[2]

[1]*Department of Chemistry, College of Education for Pure Sciences, University of Anbar, Ramadi 31001, Iraq*

[2]*Department of Chemistry, College of Science, Mustansiriyah University, Baghdad 10052, Iraq*

** **Corresponding author:***

tel: +964-7728004480
email: albajalanhanaa@uomustansiriyah.edu.iq

Received: July 22, 2023
Accepted: June 10, 2024

DOI: 10.22146/ijc.87184

Abstract: *This study focused on the development of an efficient preparation method of activated carbon for the removal of* para*-phenylenediamine (PPD) dye in an aqueous solution. Walnut shells, a readily accessible biomass source in northern Iraq, were processed into activated carbon (AC). Several techniques, such as FTIR, XRD, and SEM, were applied to describe and study the surface of AC. According to XRD analysis, all the reflection peaks with the relative intensities of various planes indicate that the obtained particle size was around 7.63 nm. The influences of contact time, adsorbent, and other variables (the thermodynamic parameters for the influence of temperature) were calculated after studying the dosage and initial concentration. The effects of the change in the acidity functions and the increasing temperature were also studied. The results found that the best adsorption occurred in 120 min, with a 0.1 g adsorbent substance weight and pH 5. The adsorption rate was at its best at a temperature of 318 K. The best-recorded adsorption rate was obtained when applying the Langmuir and Freundlich isotherms, and the adsorption processes were of a physical nature.*

Keywords: *dyes;* para*-phenylenediamine; activated carbon; walnut shells; biomass*

■ INTRODUCTION

Water is one of the basic elements for the formation of living organisms, so studying water and its investments is extremely important for the better sustainability of life in all aspects. Therefore, studying water pollution is of great importance in hydrological studies, as it is one of the important matters that has attracted the attention of scientists specialized in the field of environmental protection because this pollution leads to a disruption in the ecosystem and becomes harmful to humans, animals, or plants [1].

Water pollution is defined as a change that occurs in the natural characteristics of water, directly or indirectly, due to human activity, which makes it unfit for various uses as confirmed by the World Health Organization. Water is polluted by human, animal, plant, mineral, industrial or chemical waste, heavy metals or toxic dyes. As a result of these dyes containing *para*-phenylenediamine (PPD, $C_6H_4(NH_2)_2$), It is used as an advanced photographic agent, as a vulcanization accelerator, as an antioxidant in rubber compounds, and is also widely used in almost all hair dye ingredients [1-3]. These dangerous pollutants cause diseases in humans [4].

Pigments are colored organic compounds, synthetic or natural, that add a specific color to different substrates via applied chemical bonds [5]. Dyes are of great interest in scientific research and practical applications due to their use in textiles, printing, and paper-making. At the same time, they contribute to the pollution of rivers and waterways [6]. There are several methods to eliminate these pollutants, including electrical and chemical deposition methods, evaporation, filtration, extraction, and adsorption methods [7]. The last method was followed in this research. We need a nanomaterial represented by activated carbon (AC) because it has the properties required for the removal technology to absorb the dye.

AC is a reliable and strong adsorbent that is important for removing pollutants from water and air. AC is an organic compound with a highly porous structure that can be generated from organic raw materials (coconut shells, wood, cones, charcoal, etc.). Harmful chemical and physical processes may transfer different functions to its surface [8-9]. This work treated walnut shells (at a low cost) to get AC nanoparticles (ACNPs), which were then used to remove PPD dye from its aqueous solutions. The effects of adsorbent amount, contact time, pH, temperature, and initial concentration were examined, and the adsorption kinetics of the adsorption process were studied. Langmuir and Freundlich's models have been used to find out its equilibrium adsorption properties.

■ EXPERIMENTAL SECTION

Materials

The chemicals utilized in this study were para-phenylenediamine PPD($C_{12}H_{11}N$, HIMEDIA India), orthophosphoric acid (H_3PO_4, 85%, Fluka Garantie), hydrochloric acid (HCl, 37%, Central Drug House), sodium hydroxide (NaOH, 97%, Qualikems), and walnut shells.

Instrumentation

The instrumentations used in this work were Fourier transform infrared (FTIR, ALPHA II FTIR spectrometer, Bruker) at a range of 400 to 4000 cm^{-1} using KBr pellets, X-ray powder diffraction spectroscopy (XRD, Philips® PW 1710 diffractometer (Cu K, 40 kV/40 mA, 2 per min scanning rate)), scanning electron microscope (SEM, Carl Zeiss Microscopy Deutschland GmbH), UV-vis spectrophotometer (UV-M90, Bel Engineering), shaking water bath BS-11 (Korea), and pH meter (WTW Ph7110). A transmission electron microscope (TEM, JEOLEM-2100, Japan) was implemented to examine the size and surface morphology of ACNPs.

Procedure

Preparation of ACNPs from walnut shells

H_3PO_4 is used in a chemical activation process to create AC. The H_3PO_4 solution (20%) is diluted to 300 mL and added to 30 g of walnut shell powder, which takes 24 h. The sample was then neutralized, filtered, and dried in an oven at 60 °C for another 24 h after being washed in distilled water. After drying, the sample is allowed to cool for at least 30 min at room temperature before carbonization. The samples were heated in an electric oven at 10 °C per min. The temperature was kept at 500 °C for 3 h. Following this process, the AC was rinsed with distilled water, filtered, and dried for 24 h at 105 °C.

Adsorption experiments

As much as 0.1 g of PPD dye was dissolved in 100 mL of deionized water to prepare the standard solution at 1000 ppm. Working solutions of varying concentrations were made by diluting the standard solution. The adsorbate and sorbent suspension were agitated at 150 rpm in a water bath shaker. A UV-vis spectrophotometer was used to measure the concentration and absorbance for all solutions of the dye PPD at the maximum wavelength of 453 nm. The standard calibration curve of dye with 100–800 ppm concentrations was measured at λ_{max}.

Effect of parameters

The dye percentage removal in the adsorption experiments was conducted to measure the effects of different operating parameters. These parameters include adsorbent weight (0.01–0.10 g), contact time (15–180 min), adsorbate concentration (100–800 ppm), and pH (2–8) at various temperatures of 298, 308, and 318 K.

Conical flasks were filled with 50 mL of 5 ppm PPD and 0.1 g of the adsorbent at 318 K and then shaken in a water bath at 150 rpm for 15, 30, 45, 60, 90, 120, 150, and 180 min. After the end of the specified time, each sample was separated using a centrifuge at 4000 rpm/min speed of filtering. The filtrate was taken, and the remaining concentration was measured, and the amount of adsorption (q_e) was calculated from Eq. (1);

$$q_e = \frac{(C_0 - C_e) \times V}{m} \quad (1)$$

where C_0 and C_e are the initial and equilibrium concentrations of adsorbate (mg/L), V is the volume of the total reaction solution (L), and m is the mass of the adsorbent (g). The percentage removal of PPD dye (R%) was calculated using the Eq. (2) [10-11].

$$R\% = \frac{C_0 - C_e}{C_0} \times 100 \quad (2)$$

■ RESULTS AND DISCUSSION

FTIR Analysis

FTIR was used to analyze the surface functional groups of ACNPs at 400 to 4000 cm^{-1} using KBr pellets. Fig. S1 and Table 1 show the data FTIR spectrum used to determine which functional groups were on the surface of the adsorbent. The strong bandwidth of 3282 cm^{-1} represents the stretching vibration of the hydroxyl group. At 3009 and 831 cm^{-1}, they were referred to as the presence of C–H bonds (aromatic rings). The peaks at 2923 and 2853 cm^{-1} indicated asymmetric and symmetric stretching of CH_2 groups of alkane. A small peak at 1744 cm^{-1} was for the carbonyl groups in aldehydes, ketones, carboxylic acids, and/or lactones. The peaks at 1538 and 1453 cm^{-1} were for the aromatic rings. A sharp peak was observed at 1638 cm^{-1}, referring to the asymmetric carboxylate stretch. The detected strong peaks at 1378 and 1299 cm^{-1} belong to C–O–C groups of stretching bonds in esters and ethers. The bread peak at 1058 cm^{-1} refers to R–OH vibration groups in primary and secondary alcohols [12-15].

XRD Analysis

Powder XRD was used to obtain information about the structure, phase, composition, shape, size, and crystallinity of the prepared nanostructured activated carbon. The XRD profile of the AC is shown in Fig. S2. The lack of a sharp peak indicates a mostly amorphous structure in this AC, which exhibits extremely broad diffraction peaks [16]. The spectra had three broad diffraction peaks at 2 = 24°, 29°, and 43°, which belong to the diffraction of (0 0 2), (1 0 1), and (1 0 2), respectively. At 500 °C activation temperature, the peak appears at around 24°, indicating a more regular crystalline structure and improved layer alignment [17]. In this investigation, the average crystallite size of AC-NPs was calculated to be 7.63 nm.

SEM and TEM Analysis

SEM was implemented to examine the surface morphology and the pore size of the obtained ACNPs. A SEM image of unmodified AC is shown in Fig. 1(a). The surface is even and has few pores. According to Mohanty et al. [18], some salt particles are scattered across the surface of the AC due to the residual phosphate or other metal compounds. Excess dehydrated acid might build a protective layer that blocks out the impact of the surrounding atmosphere and further restricts the natural formation of inner porosity [19]. These particles

Table 1. The data for FTIR analysis of ACNPs

Wavenumber (cm^{-1})	Vibrational mode
3282	O–H bond stretching
3009 and 831	C–H bonds (aromatic rings)
2923 and 2853	CH_2 stretching of alkane
1744	carbonyl groups
1538 and 1453	aromatic rings
1638	carboxylate stretch
1378 and 1299	C–O–C stretching
1058	R–OH vibration

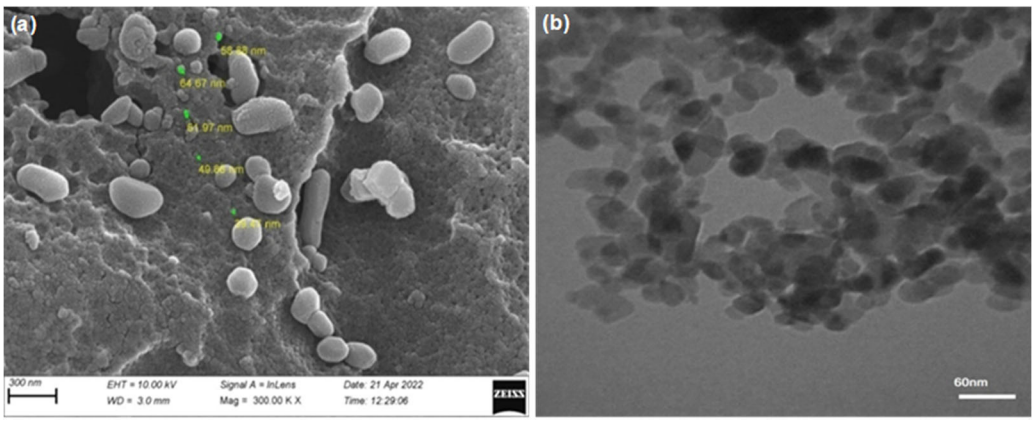

Fig 1. (a) SEM and (b) TEM micrographs of the ACNPs after carbonization at 500 °C

could block PPD from entering the pores. The adsorption capacity of the target pollutants may be improved, according to Mohanty et al. [18]. The form and size of the nanoparticles shown in Fig. 1(b) were identified by the TEM. The green synthesis method of synthesizing ACNPs resulted in irregularly shaped (almost spherical) nanocrystals around 40-60 nm in size.

Adsorption Results

Effect of contact time

The contact time study for the PPD dye adsorption on the ACNPs was investigated as a function of the removal efficiency of PPD at pH 5. As much as 50 mL of PPD was prepared at a concentration of 100 ppm by adding 0.1 g of the adsorbent and putting it in a water bath shaker at 15 to 180 min intervals. As shown in Fig. 2(a), the result of the experiments showed that the R% of the dye from its aqueous solution increased with an increasing contact time of about 120 min. After that, it almost became constant at 180 min. Thus, a maximum of R% reached equilibrium at 120 min and was used in all subsequent experiments.

Effect of initial concentration

Several initial concentrations between 100 and 800 ppm at 813 K, pH 5, equilibrium time at 120 min, and 0.1 g of the adsorbent were utilized to determine the influence of PPD concentration on the adsorption. The results in Fig. 2(b) indicate that removal efficiency decreases when the initial concentrations of PPD increase. This increase is due to active sites on the adsorbent surface that were sufficient for PPD dye adsorption. The active sites include OH, COOH, and aromatic rings. As a result, residual PPD remained in an aqueous solution at high initial concentrations [14,20-21].

Effect of temperature

PPD dye solutions with a volume of 50 mL and a concentration of 100 ppm were prepared to evaluate the impact of temperature on adsorption. A total of 0.1 g of

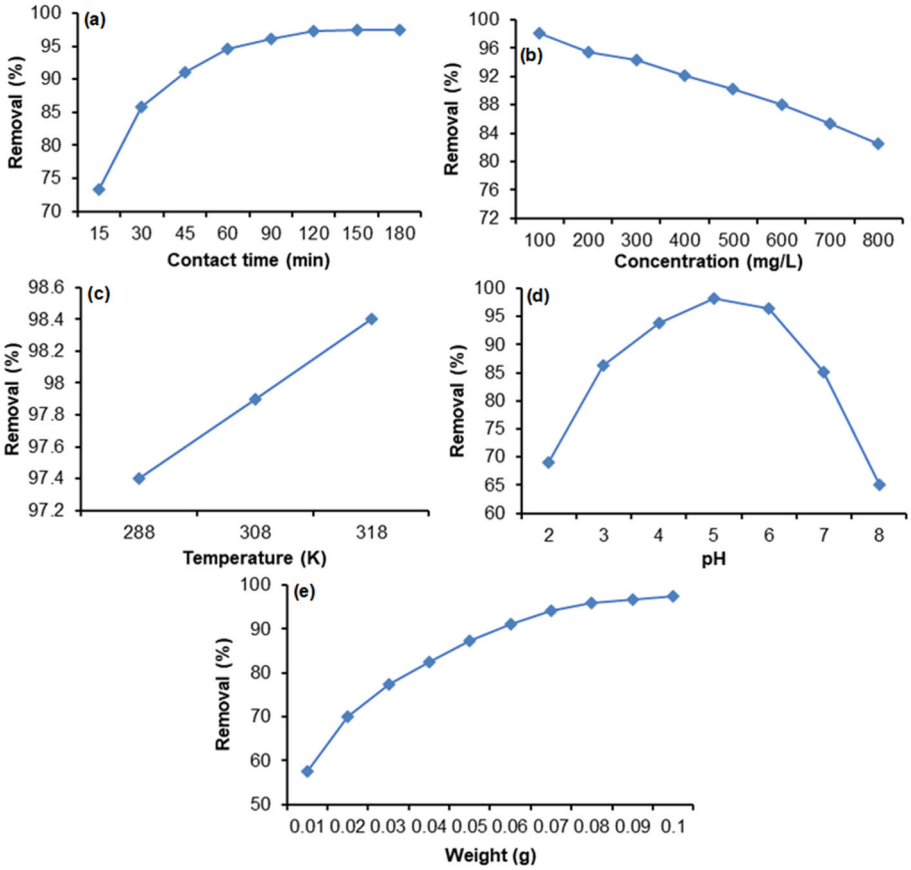

Fig 2. The effect of (a) equilibrium time, (b) initial concentration, (c) temperature, (d) pH, and (e) adsorbent dosage

the ACNPs was added and then placed in a water bath shaker at different temperatures of 298, 308, and 318 K for 120 min. Fig. 2(c) can be used to conclude this effect, which shows that the removal efficiency R% increased with the temperature increase. The change in dye molecules' kinetic energy, the pores size, and the increase in diffusion velocities due to increased temperature increased the removal efficiency. Thus, this adsorption is an endothermic process [20,22].

Effect of pH

The adsorption studies were continued by investigating the effect of pH on the PPD adsorption on the ACNPs. Several solutions with a volume of 50 mL and a concentration of 100 ppm of PPD dye were prepared, and 0.1 g of the ACNPs were added at 318 K in a water bath shaker for 120 min. This experiment series was accompanied by a change in pH values of 2, 3, 4, 5, 6, 7, and 8. Several properties are affected by the pH during the adsorption process, such as active sites by break up on the functional groups on the adsorbent, the surface charge of the adsorbent, and the chemical properties of the dye solution [22].

The results shown in Fig. 2(d) are an increase in R% with a decrease in pH value from 2 to 5. In contrast, at pH values from 6 to 8, there was a decrease in R% values. The best R% was at pH 5 because at high acidity, there is the possibility of reverse redox processes and the formation of the ion (A) in Scheme 1(a) [23]. It causes repulsion with H^+ ions on the adsorbent and prevents its adsorption. At low acidity, due to the high concentration of OH^- ions in the solution, it leads to the formation of the ion (B) in Scheme 1(b) [24], which leads to the generation of repulsion forces with OH^- ions present on the adsorbent, so the value of R% decreases.

Adsorbent dosage effect

Adsorbent dosage plays an essential role in dye adsorption. Various amounts of ACNPs were used from 0.01 to 0.10 g, added to several PPD dye solutions with 100 ppm in 50 mL in a water bath shaker at 318 K for 120 min (pH 5) to indicate the adsorbent dosage effect on PPD adsorption. Fig. 2(e) showed experimental results that the R% increased with the increase in adsorbent dosage. This is caused by the increased availability of the active sites on the adsorbent surface, which can react with the active sites on the dye [20,22,25].

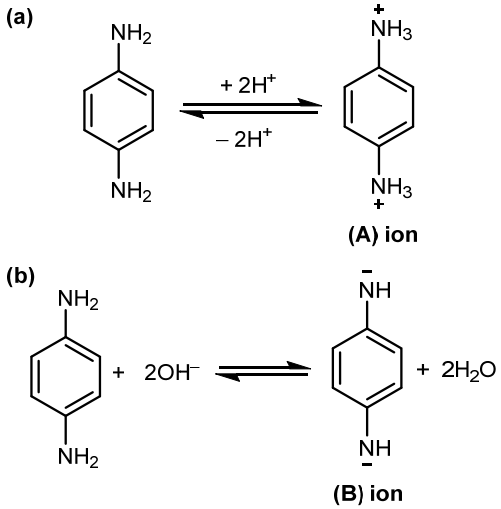

Scheme 1. The mechanism formation of (A) and (B) ions

Adsorption Isotherm

The adsorption isotherm was studied to investigate the division of adsorbate molecules in an equilibrium state and the homogeneity and heterogeneity of the adsorbent surface [26]. The isotherm types used in this study are Langmuir and Freundlich for the adsorption process, with an initial concentration of PPD dye of 100 to 800 ppm at a contact time of 120 min. Eq. (3) and (4) were used to determine the results of adsorption isotherms, as shown in Table 2 and Fig. 3(a) and (b):

$$\frac{C_e}{q_e} = \frac{1}{K_l q_m} + \frac{C_e}{q_m} \quad (3)$$

$$\ln q_e = \ln K_f + \left(\frac{1}{n}\right) \ln C_e \quad (4)$$

where q_e is the amount adsorbed of dye (mg/g), and C_e is the equilibrium concentration of PPD dye in the adsorption solution (ppm).

The plot C_e/q_e vs C_e gives the maximum adsorption capacity value (q_m, mg/g) from the slope. The Langmuir constant (K_l, L/mg) is obtained from the intercept. While the plot ln q_e vs ln C_e gives the adsorption intensity constant (1/n) from the slope and Freundlich constant, (K_f, L/g) from the intercept [26-27]. The values of the constants, parameters, and linear correlation coefficient (R^2) are deduced in Table 3. It was indicated from the R^2 values of the Langmuir isotherm was better

Table 2. The results of adsorption isotherms

C_0 (ppm)	C_e (ppm)	Q_e (mg/g)	C_e/Q_e ($\times10^{-5}$)	Ln C_e	Ln Q_e
100	2.6	48700	5.3	0.9	10.8
200	9.0	95500	9.4	1.6	11.5
300	17.4	141300	12.3	2.9	11.9
400	29.5	185250	15.9	3.4	12.1
500	47.8	226100	21.1	3.9	12.3
600	71.6	264200	27.1	4.3	12.5
700	102.4	298800	34.3	4.6	12.6
800	143.7	328150	43.8	5.0	12.7

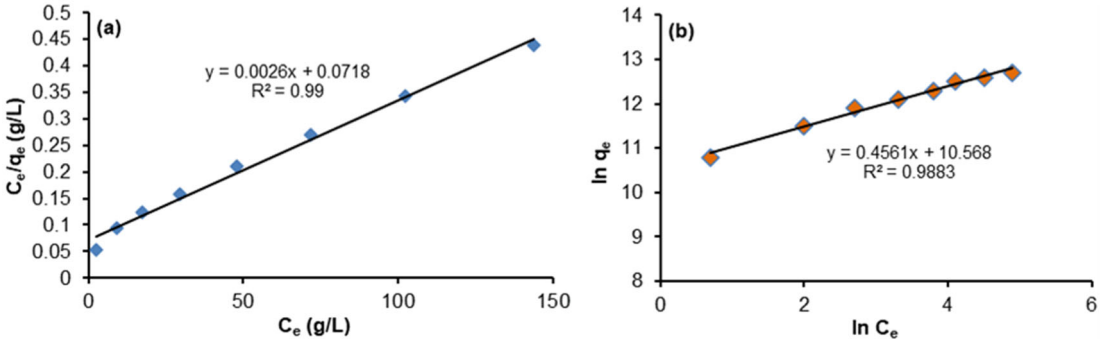

Fig 3. (a) Langmuir and (b) Freundlich isotherm models

Table 3. The values of all constants for Langmuir and Freundlich isotherms

Isotherm quantities	Langmuir			Freundlich		
	R^2	q_{max} ($\times10^3$)	k_l	R^2	n	k_f
Values	0.990	384.6	0.036	0.989	2.1	34682

than the Freundlich isotherm for the adsorption process for dye removal, assuming the dye coverage on the ACNPs was a monolayer with the homogenous division on the surface of the adsorbent.

Adsorption Kinetics

The study of adsorption kinetics is useful in knowing the bonding state of adsorbed particles on the surface. This interest justifies conducting many studies on the adsorption kinetics of its different systems. In this work, two models of kinetics were employed to indicate the kinetics of PPD dye adsorption by ACNPs, the pseudo-first-order and the pseudo-second-order models, which were formulated as Eq. (5) and (6), respectively [11,22].

$$\ln(q_e - q_t) = \ln q_e - k_1 t \quad (5)$$

In this equation, q_e and q_t are the adsorption amounts of dye on the adsorbed (mg/g) at equilibrium and at any time t (min). The plot of ln (q_e – q_t) vs. t affords the rate constant of first order (k_1, min^{-1}) from the slope and gives the q_e value from the intercept, as shown in Fig. 4(a). The second-order rate constant (k_2, g/mg. min^{-1}) and the q_e value were obtained from its intercept and slope, respectively, as shown in Fig. 4(b).

$$\frac{t}{q_e} = \frac{1}{k_2 q_e^2} + \frac{1}{q_e} \quad (6)$$

Table 4 lists the obtained results after applying the pseudo-first-order model. Although R^2 is relatively high (0.9946), it cannot apply a pseudo-first-order equation due to the large discrepancy between the theoretical and experimental values of q_e (19610 and 48700 mg/g, respectively). It was observed that the theoretical value of q_e (50000) and the experimental value (48700) converged very well using the pseudo-second-order equation. Furthermore, the value of R^2 was 1, indicating that the predicted values were consistent with the measured ones

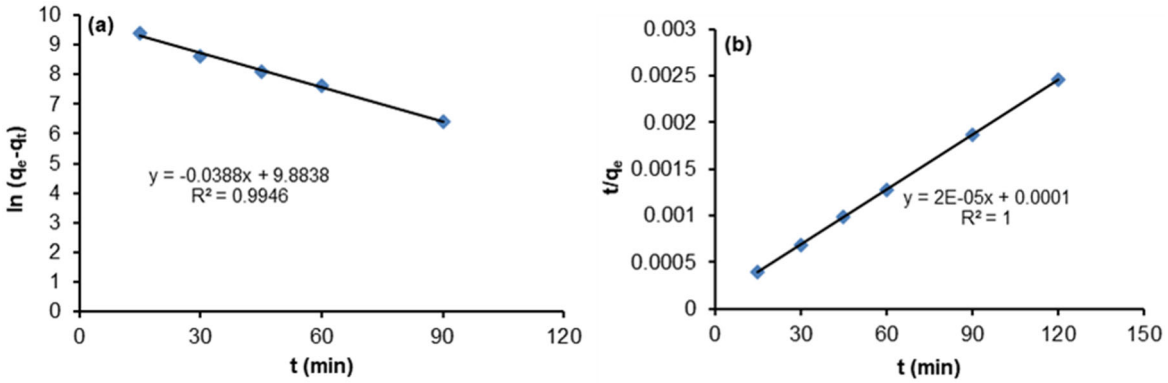

Fig 4. (a) Pseudo-first-order and (b) pseudo-second-order kinetic models

Table 4. Pseudo-first- and second-order constants

Constants	Values	
	Pseudo-first-order	Pseudo-second order
R^2	0.9946	1.00
K	0.039 min^{-1}	4×10^{-6} g/mg.min^{-1}
q_e experimental (mg/g)	48700	48700
q_e theoretical (mg/g)	19610	50000

Hence, pseudo-second-order kinetics govern the PPD dye adsorption.

Adsorption Thermodynamics

This part reflects the thermodynamic quantities and the spontaneous nature of the adsorption process. These quantities can be calculated in terms of free energy (ΔG°), enthalpy (ΔH°), and entropy (ΔS°) using the equilibrium constant that changes with temperature. The relationship of the equilibrium constant (k_e) is given in Eq. (7) [28-29]:

$$k_e = C_{Ae}/C_e \quad (7)$$

where C_{Ae} represents the amount of adsorbed on the adsorbent surface (mg/L), respectively. The thermodynamic magnitudes are calculated from Eq. (8–10) [29-30].

$$\Delta G° = -RT \ln k_e \quad (8)$$

$$\Delta G° = \Delta H° - T\Delta S° \quad (9)$$

$$\ln k_e = \frac{\Delta S°}{R} - \frac{\Delta H°}{RT} \quad (10)$$

The effect of temperature on the PPD dye adsorption on the ACNP powder surface was studied at temperatures of 298, 308, and 318 K. The results are recorded in Table 5, which shows the thermodynamic functions of dye adsorption. When plotting the values of ln k_e vs 1/T a straight line is obtained, as in Fig. 5. The value of ΔH° and ΔS° was calculated from the slope and intercept of the plot, respectively. The negative of ΔG° values reflects that the adsorption process is spontaneous. The enhanced dye adsorption process is shown by a drop in ΔG° values with increasing temperature. The positive

Table 5. The thermodynamic constants

T/K	ΔG (kJ/mol)	ΔH (kJ/mol)	ΔS (kJ/mol)
298	−24.5		
308	−25.7	+13.7	+127.9
318	−27.0		

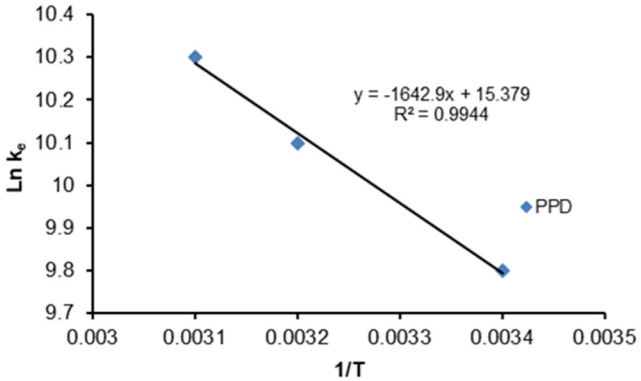

Fig 5. Plot of ln k_e vs 1/T for PPD adsorption on the ACNPs

value of ΔH° confirms that the PPD adsorption is an endothermic process and indicates the nature of adsorption is physisorption due to the low value of ΔH° (13.7 kJ/mol) (ΔH° < 20 kJ/mol is physisorption, and ΔH° > 40 kJ/mol is chemisorption). A positive value of ΔS° indicates an increase in randomness at the solid-solution system interface [28-29].

■ CONCLUSION

In this work, low-cost nano-AC was prepared from locally available walnut shells by a chemical activation process. The necessary analyses were conducted for this nano-powder, such as XRD, FTIR, SEM and TEM, to use it as an adsorbent surface for PPD dye from its aqueous solution. The XRD showed that the particle size was around 7.63 nm, as determined by the reflection peaks and relative intensities of different planes. FTIR results showed most of the active groups on the adsorbent surface since the adsorption process is affected by several factors such as initial concentration, temperature, contact time, and pH. Therefore, the effect of these factors was studied and other factors (the thermodynamic parameters for the influence of temperature) were computed. Also, clarify the adsorption kinetics. The best adsorption was reported to occur in 120 min with 0.1 g of adsorbent material and pH 5. At 318 K, the adsorption rate was optimal. The Langmuir and Freundlich isotherms produced the highest adsorption rate. The efficiency of the prepared adsorbent surface in the dye adsorption process was demonstrated when compared with what was mentioned in the references.

■ ACKNOWLEDGMENTS

We would like to appreciate and thank both the staff and team of Department of Chemistry, College of Education for Pure Sciences, University of Anbar, Ramadi, Iraq and also the Department of Chemistry, College of Science, Mustansiriyah University, Baghdad, Iraq, for supporting us until this work become an article to benefit the research field.

■ CONFLICT OF INTEREST

The authors have no conflict of interest.

■ AUTHOR CONTRIBUTIONS

Hanaa Hassan Hussein suggested the research idea and conducted the experiment, Shahbaa Fayyad Bdewi performed calculations and graphs, and Shireen Abdulmohsin Azeez wrote and revised the manuscript. All authors agreed to the final version of this manuscript.

■ REFERENCES

[1] Khasanova, S., Alieva, E., and Shemilkhanova, A., 2023, Environmental Pollution: Types, Causes and Consequences, *BIO Web Conf.*, 63, 07014.

[2] IARC Working Group on the Evaluation of the Carcinogenic Risk of Chemicals to Man, 1978, *IARC Monographs on the Evaluation of the Carcinogenic Risk of Chemicals to Man: Some Aromatic Amines and Related Nitro Compounds-Hair Dyes, Colouring Agents and Miscellaneous Industrial Chemicals*, IARC, Lyons, France.

[3] Hansen, J., Møllgaard, B., Avnstorp, C., and Menné, T., 1993, Paraben contact allergy: Patch testing and *in vitro* absorption/metabolism, *Am. J. Contact Dermatitis*, 4 (2), 78–86.

[4] Lin, L., Yang, H., and Xu, X., 2022, Effects of water pollution on human health and disease heterogeneity: A review, *Front. Environ. Sci.*, 10, 880246.

[5] Papadakis, R., 2021, *Dyes and Pigments: Novel Applications and Waste Treatment*, IntechOpen, Rijeka, Croatia.

[6] Chowdhary, P., Bharagava, R.N., Mishra, S., and Khan, N., 2020, "Role of Industries in Water Scarcity and its Adverse Effects on Environment and Human Health" in *Environmental Concerns and Sustainable Development: Volume 1: Air, Water and Energy Resources*, Eds. Shukla, V., and Kumar, N., Springer Singapore, Singapore, 235–256.

[7] Mohamed, A.R., Hussein, H.H., and Sirhan, M., 2022, Removal of PPD dye from its aqueous solution by adsorption using the cadmium oxide nanoparticles, *Bull. Natl. Inst. Health Sci.*, 140 (02), 1915–1929.

[8] Roquia, A., khalfan hamed Alhashmi, A., and hamed Abdullah alhasmi, B., 2021, Synthesis and

characterisation of carbon nanotubes from waste of *Juglans regia* (walnut) shells, *Fullerenes, Nanotubes Carbon Nanostruct.*, 29 (11), 860–867.

[9] Tadda, M.A., Ahsan, A., Shitu, A., El Sergany, M., Arunkumar, T., Jose B., Razzaque, M., and Nik Daud, N.N., 2016, A review on activated carbon: Process, application and prospects, *J. Adv. Civ. Eng. Pract. Res.*, 2 (1), 7–13.

[10] Azeez, S.A., Hussein, F.M., and Al-Saedi, R.W.M., 2023, Adsorption isotherms for CBY 3G-P dye removal from aqueous media using TiO_2 Degussa, Fe_2O_3, and TiO_2/(DPC), *Indones. J. Chem*., 23 (3), 702–715.

[11] Sharma, G., Sharma, S., Kumar, A., Lai, C.W., Naushad, M., Shehnaz, S., Iqbal, J., Stadler, F.J., and Igwegbe, C.A., 2022, Activated carbon as superadsorbent and sustainable material for diverse applications, *Adsorpt. Sci. Technol.*, 2022, 4184809.

[12] Lach, J., Ociepa-Kubicka, A., and Mrowiec, M., 2021, Oxytetracycline adsorption from aqueous solutions on commercial and high-temperature modified activated carbons, *Energies*, 14 (12), 3481.

[13] Li, X., Qiu, J., Hu, Y., Ren, X., He, L., Zhao, N., Ye, T., and Zhao, X., 2020, Characterization and comparison of walnut shells-based activated carbons and their adsorptive properties, *Adsorpt. Sci. Technol.*, 38 (9-10), 450–463.

[14] Kunusa, W.R., Iyabu, H., and Abdullah, R., 2021, FTIR, SEM and XRD analysis of activated carbon from sago wastes using acid modification, *J. Phys.: Conf. Ser.*, 1968 (1), 012014

[15] Allwar, A., 2016, Preparation and characteristics of activated carbon from oil palm shell for removal of iron and copper from patchouli oil, *Int. J. Appl. Chem.*, 12 (3), 183–192.

[16] Wang, S., and Lu, G.Q., 1997, Effects of oxide promoters on metal dispersion and metal–support interactions in Ni catalysts supported on activated carbon, *Ind. Eng. Chem. Res.*, 36 (12), 5103–5109.

[17] Kasaoka, S., Sakata, Y., Tanaka, E., and Naitoh, R., 1989, Preparation of activated fibrous carbon from phenolic fabric and its molecular-sieve properties, *Int. Chem. Eng.*, 29 (1), 101–114.

[18] Mohanty, K., Das, D., and Biswas, M.N., 2005, Adsorption of phenol from aqueous solutions using activated carbons prepared from *Tectona grandis* sawdust by $ZnCl_2$ activation, *Chem. Eng. J.*, 115 (1), 121–131.

[19] Girgis, B.S., and Ishak, M.F., 1999, Activated carbon from cotton stalks by impregnation with phosphoric acid, *Mater. Lett.*, 39 (2), 107–114.

[20] Gorzin, F., and Bahri Rasht Abadi, M.M., 2018, Adsorption of Cr(VI) from aqueous solution by adsorbent prepared from paper mill sludge: Kinetics and thermodynamics studies, *Adsorpt. Sci. Technol.*, 36 (1-2), 149–169.

[21] Al-Massaedh, A.A., and Khalili, F.I., 2021, Removal of thorium(IV) ions from aqueous solution by polyacrylamide-based monoliths: equilibrium, kinetic and thermodynamic studies, *J. Radioanal. Nucl. Chem.*, 327 (3), 1201–1217.

[22] Arnata, I.W., Suprihatin, S., Fahma, F., Richana, N., and Sunarti, T.C., 2019, Adsorption of anionic Congo red dye by using cellulose from sago frond, *Pollut. Res.*, 38 (3), 557–567.

[23] Meyer, A., and Fischer, K., 2015, Oxidative transformation processes and products of para-phenylenediamine (PPD) and *para*-toluenediamine (PTD), A review, *Environ. Sci. Eur.*, 27 (1), 11.

[24] Rosenberg, D., Pansegrau, S., Wachholz, M., Köppen, A., Busker, A., and Jansen, W., 2018, Organic redox-flow batteries using hair dyes and pharmaceuticals, *World J. Chem. Educ.*, 6 (1), 63–71.

[25] Wang, J., Wang, R., Ma, J., and Sun, Y., 2022, Study on the application of shell-activated carbon for the adsorption of dyes and antibiotics, *Water*, 14 (22), 3752.

[26] Omidi-Khaniabadi, Y., Jafari, A., Nourmoradi, H., Taheri, F., and Saeedi, S., 2015, Adsorption of 4-chlorophenol from aqueous solution using activated carbon synthesized from aloe vera green wastes, *J. Adv. Environ. Health Res.*, 3 (2), 120–129.

[27] Koffi, A.L.C., Akesse, D.P.V., Kouyate, A., Dongui, B.K., and Yao, K.B., 2022, Adsorption of methylene blue on MnO_2-modified activated carbon prepared

from cocoa pod shells, *Int. J. Res. Rev.*, 9 (10), 34–42.

[28] Hami, H.K., Abbas, R.F., Azeez, S.A., and Mahdi, N.I., 2021, Azo dye adsorption onto cobalt oxide: Isotherm, kinetics, and error analysis studies, *Indones. J. Chem*., 21 (5), 1148–1157.

[29] Hamooshy, E.A., and Hussein, H.H., 2021, Thermodynamic properties study of dissolution of 2-hydroxbenzoic acid in binary solvent (ethanol+ water) at various temperatures, *Egypt. J. Chem.*, 64 (11), 6499–6504.

[30] Alalaw, N.K.M., Hamooshy, E.A., and Hussein, H.H., 2022, Thermodynamic study of the solubility of guanine and uracil in deferent aqueous sugar solution, *Egypt. J. Chem.*, 65 (4), 371–376.